Accuracy Comparison of High-Order Finite Difference Schemes for the Evolution of Two-Dimensional Finite-Amplitude Disturbances

J.M.M. Sousa* C.F.N.B. Silva J.C.F. Pereira

Abstract

Direct simulations of small- and finite-amplitude disturbances in spatially periodic plane Poiseuille flow were performed. The ability of three high-order finite difference methods to predict the proper behavior of the disturbances was under investigation. The proposed procedure allowed to conclude about the spatial resolution and time-step required by those schemes to produce numerically accurate results.

Key words: high-order schemes, finite differences, finite-amplitude stability.

AMS subject classifications: 35A40, 35B20, 65P20.

1 Introduction

During the last years, an increasing number of Navier-Stokes solvers has been reported with which unsteady flow solutions have been sought. Most of these numerical schemes are at least second-order accurate (based on local truncation analysis), which is accepted to be a minimum requirement for any numerical scheme purporting to perform physically meaningful unsteady simulations [3]. Irrespectively, difficulties arise when aiming to assess the accuracy of the numerical predictions making use of available results on unsteady fluid flow. Similar problems concerning the numerical solution errors and their estimation assume even stronger significance in large-eddy simulations (LES). In the context of LES, so that effective testing of subgrid-scale models can be achieved, one must be able to separate the issue of numerical scheme accuracy and the evaluation of the subgrid-scale model assumptions.

Spectral methods are the most natural option for a numerical scheme to carry out the above mentioned simulations, because of the high accuracies of these methods. However, finite-difference schemes present easier implementation and extension to complex geometries, despite that their accuracy level is often inadequate. To investigate the ability of established finite difference methods to provide the correct description (concerning damping and phase accuracy) of relevant standard problems is, therefore, a subject of great relevance. With this goal in mind, the problem of the evolution of finite-amplitude disturbances seems to be an appropriate background to enable such investigations to generate significant information on the effectiveness of the numerical methods, when these are applied to real situations ranging from hydrodynamic instability to turbulent flow simulations.

It must be mentioned that the issue of finite-amplitude stability has been the object of systematic investigations. Among these we emphasize the work of Fasel [4], Orszag and Patera [13, 14], and Orszag and Kells [12], deeming the problems of boundary layer, plane Poiseuille and Couette flows. See also Patera and Orszag [15] for the case of pipe flow. In earlier years, limited computer resources have forced other researchers to the use of approximate methods. However, reliable results have been provided, e.g., by George and Hellums [6], for the case of two-dimensional plane Poiseuille flow.

The present work presents a methodical evaluation of the performance of finite difference schemes in which the two-dimensional Navier-Stokes results reported by George *et al.* [7] have been used as a reference for the transient behavior of finite-amplitude disturbances. There is not any *a priori* excuse for the choice of a two-dimensional test case. However, as pointed out by Jiménez [8], two-dimensional cases are simpler to compute and still relevant understanding can be gained from such analyses. In Section 2, the governing equations and the numerical schemes

*Instituto Superior Tecnico, Technical University of Lisbon, Mechanical Engineering Department, Av. Rovisco Pais, 1096 Lisboa Codex, Portugal.

ICOSAHOM'95: Proceedings of the Third International Conference on Spectral and High Order Methods. ©1996 Houston Journal of Mathematics, University of Houston.

are described. The following temporal discretizations were employed: quadratic Leith, Crank-Nicholson and Adams-Bashforth. These discretizations were used together with third-order (using quadratic upstream interpolation) and fourth-order (fifth-order upwind-biased approximations for the convective terms only) spatial accuracy. In Section 3, a careful characterization of the test cases (including validation *via* linear stability theory) is given. The last two sections report the results and main findings of the present study.

2 Numerical formulation

2.1 Governing equations

The conservative form of the continuity and momentum equations for incompressible flow, expressed in Cartesian coordinates (x,y) with corresponding velocity components (u,v) and p the pressure, are given by

$$u_x + v_y = 0 \tag{1}$$

$$u_t + (uu)_x + (vu)_y = -p_x + \frac{1}{Re}(u_{xx} + u_{yy}) \tag{2}$$

$$v_t + (uv)_x + (vv)_y = -p_y + \frac{1}{Re}(v_{xx} + v_{yy}), \tag{3}$$

where subscripts indicate partial differentiation, the Reynolds number $Re = \frac{u_o h}{\nu}$, with u_o standing for a characteristic velocity, h for a characteristic length and ν for the kinematic viscosity.

The primitive equations (1) - (3) will be integrated in time by the well known pressure-correction method which requires the solution of a Poisson equation. A staggered grid system will be used for the discretization of the governing equations. In the presence of solid boundaries, no-slip conditions will be imposed for velocities. All the algorithms to be presented here are based on a conservative control-volume formulation.

2.2 Discretization schemes

Finite difference methods intended to investigate problems involving hydrodynamic stability and transition or the simulation of turbulent flows have to meet a number of requirements in order to ensure successful calculations [3]. It is known that, when solutions are of periodic nature, the numerical method must be at least second-order accurate (including initial and boundary conditions), based on local truncation analysis [2]. However, spatial second-order accuracy may still be inadequate for the above mentioned simulations to be performed using realistic computational grid sizes [17]. The migration of those schemes to higher order of accuracy, although desirable, brings along the issue of stability. High-order accurate finite difference methods are often plagued by numerical instability, taking the form of unphysical oscillations which corrupt the expected solution. Nevertheless, the lack of robustness exhibited by such methods may be combated. Employing high-order upwind-biased finite difference schemes, the undesirable non-physical effects such as artificial viscosity may be excluded or at least minimized to acceptable level, while its basic stable convective sensitivity property is retained. In order to enable the investigation of physical instabilities (unstable waves), the transient character of the flowfield must also be resolved accordingly. Further, Fasel [4] indicates that second-order accuracy for time derivatives is an additional requirement.

In the next paragraphs a succint description of the discretization schemes used in the reported calculations is given.

Scheme A employs the third-order accurate QUICK formulas [9] to approximate the convective terms occurring in equations (2) and (3). A three-point upstream-weighted quadratic interpolation is used to obtain each grid cell wall value individually, in accordance to a conservative formulation. The consistent treatment of the diffusion is equivalent to central differencing. A Leith-type of temporal discretization is also employed, making use of Lagrangian integrals to derive the finite difference expressions, as shown by Leonard [9]. The resulting explicit formula for convection and diffusion, for example in the one-dimensional case with $u_i > 0$ is given by

$$\begin{aligned} u_i^{n+1} &= u_i^n - \tfrac{1}{2}C(u_{i+1}^n - u_{i-1}^n) \\ &+ (\gamma + \tfrac{1}{2}C^2)(u_{i+1}^n - 2u_i^n + u_{i-1}^n) \\ &+ C(\tfrac{1}{6} - \gamma - \tfrac{1}{6}C^2) \\ &\times (u_{i+1}^n - 3u_i^n + 3u_{i-1}^n - u_{i-2}^n), \end{aligned} \tag{4}$$

where C is the Courant number, γ denotes the non-dimensional diffusion coefficient and the superscripts indicate the time level. The use of quadratic upstream interpolation allows to obtain third-order truncation error in time, as long as Re remains high. Further details for the application of this method, known as QUICKEST, to two-dimensional fluid flow problems, were given by Pereira and Sousa [16].

In scheme B, the convective terms are also approximated using the third-order accurate QUICK finite difference formulas and the diffusion terms are discretized

using second-order accurate central differencing. However, in this case, the simulations advance the variables in time using the second-order accurate implicit Crank-Nicholson time-stepping method for the viscous terms, while the second-order accurate explicit Adams-Bashforth method is applied to convective terms. Once again, for the one-dimensional case with $u_i > 0$ one may write

$$(5)\ u_i^{n+1} = u_i^n + \tfrac{1}{2}(3H_i^n - H_i^{n-1}) + \tfrac{1}{2}(M_i^{n+1} + M_i^n)$$

$$(6)\quad \begin{aligned} H_i^n &= \tfrac{C}{8}(3u_{i+1}^n + 3u_i^n - 7u_{i-1}^n + u_{i-2}^n) \\ M_i^n &= \gamma(u_{i+1}^n - 2u_i^n + u_{i-1}^n). \end{aligned}$$

Scheme C employs high-order finite difference approximations for all terms arising in the set of equations (1) - (3). The algorithm is explicitly advanced in time using the second-order accurate Adams-Bashforth method. First-order accuracy on the viscous terms is tolerated because the problems to be investigated are at large Re. Similarly to the aforementioned schemes, one may write

$$(7)\qquad u_i^{n+1} = u_i^n + \tfrac{1}{2}(3H_i^n - H_i^{n-1}) + M_i^n.$$

Here the convective terms H_i are approximated using fifth-order accurate upwind-biased differences. The first-order derivatives arising in the non-linear terms are discretized using seven-point stencils, originating the corresponding discrete contributions to H_i. For example, in the one-dimensional case with $u_i > 0$, one writes

$$(8)\left[\frac{\partial u}{\partial x}\right]_i \sim \frac{-6u_{i+2}+60u_{i+1}+40u_i-120u_{i-1}+30u_{i-2}-4u_{i-3}}{120\triangle x}.$$

The finite difference contributions to the diffusive terms M_i, arising from the second-order derivatives, are obtained using fourth-order central differences approximations as

$$(9)\qquad \left[\frac{\partial^2 u}{\partial x^2}\right]_i \sim \frac{-u_{i+2}+16u_{i+1}-30u_i+16u_{i-1}-u_{i-2}}{12\triangle x^2}.$$

The pressure gradient terms in equations (2) and (3) are also discretized using high-order finite differences. Fourth-order of accuracy was required for the approximation of first-order derivatives, but one should note the implications of using a staggered grid system, yielding

$$(10)\qquad \left[\frac{\partial p}{\partial x}\right]_{i-\frac{1}{2}} \sim \frac{-p_{i+1}+27p_i-27p_{i-1}+p_{i-2}}{24\triangle x}.$$

The divergence operator arising in equation (1) may be obtained by the application of the finite difference approximation to a first-order derivative in each spatial direction. Requiring fourth-order accuracy, the central differencing formula reads

$$(11)\qquad \left[\frac{\partial u}{\partial x}\right]_i \sim \frac{-u_{i+2}+8u_{i+1}-8u_{i-1}+u_{i-2}}{12\triangle x}.$$

Scheme C also employs a fourth-order accurate discretization of the Poisson equation that arises in all these numerical schemes using the pressure correction method.

It should be mentioned that, due to the staggered grid arrangement, the u and v velocity components are sometimes required at locations where they are not available. For consistency, a cubic interpolation technique based on Lagrange polynomial method, which is fourth-order accurate, is used.

Near solid boundaries the overall accuracy of the method is reduced. Grid points lying next to the boundaries where no-slip conditions are imposed, are treated using either second-order accurate finite difference stencils (pressure gradient and viscous terms, and both the divergence and Laplacian operators) or a third-order accurate upwind-biased scheme (convective terms) which may be written as

$$(12)\qquad \left[\frac{\partial u}{\partial x}\right]_i \sim \frac{2u_{i+1}+3u_i-6u_{i-1}+u_{i-2}}{6\triangle x},$$

for the one-dimensional case with $u_i > 0$.

3 Test cases

Aiming to evaluate the accuracy and robustness of the numerical schemes presented in the previous section, two test cases are carefully described here.

3.1 Small-amplitude disturbances

The first test case consists in the calculation of the evolution of small-amplitude disturbances in channel flow. It is our ultimate objective to make available numerical schemes which are able to accurately perform the simulation of finite-amplitude disturbances. However, before committing oneself to carry out this kind of simulations, the above referred methods must be applied to a closely related problem allowing results validation. In the case of small- amplitude disturbances, exact solutions are available from linear stability theory (LST).

The flowfield is initialized as

$$(13)\qquad \begin{aligned} u(x,y,t) &= 1 - y^2 - \varepsilon\tilde{u} \\ v(x,y,t) &= \varepsilon\tilde{v}, \end{aligned}$$

where $(\tilde{u}, \tilde{v})$ represent an eigensolution of the Orr-Sommerfeld equation for $Re = 7500$ and wavenumber $\alpha = 1.00$. The parameter ε defines the amplitude of the disturbance and therefore it must be small. The value of $\varepsilon = 0.001$ has been used. A supercritical Reynolds number ($Re > Re_c, Re_c = 5772.22$ with $\alpha = 1.02$ [11]) has been chosen in order to investigate the ability of the numerical schemes to describe the behavior of linearly unstable

disturbances. As a basis for the comparison with the eigensolution, the energy associated to the perturbation in the channel is computed at each time step. It may be defined as

$$E(t) = \int_{-1}^{1} \int_{0}^{2\pi/\alpha} (\tilde{u}^2 + \tilde{v}^2)\, dx\, dy, \tag{14}$$

and the monitorization of the quantity $\frac{E}{E_0}$, where $E_0 = E(t = 0)$, allows to assess the accuracy of the employed schemes. In accordance to LST, $\frac{E}{E_0}$ is expected to grow in time as $e^{2\sigma t}$, where $\sigma = 0.002235$ [10]. It is further envisaged that this preliminary test will indicate the adequate numerical grid sizes to be used later in the simulation of finite-amplitude disturbances.

3.2 Finite-amplitude disturbances

The second test case comprises the development of an initial disturbance which was also superimposed to the fully developed laminar channel flow solution, analogously to what expressed by equation (13). However, in this case, the perturbation takes the following form

$$\begin{aligned} \tilde{u}(x,y) &= \varepsilon f_y(a,y)\cos(\alpha x) \\ \tilde{v}(x,y) &= \varepsilon \alpha f(a,y)\sin(\alpha x), \end{aligned} \tag{15}$$

where $f(a,y)$ is a function given by

$$f(a,y) = f^* \left[\frac{\cosh(ay)}{\cosh(a)} - \frac{\cos(ay)}{\cos(a)} \right], \tag{16}$$

with $\varepsilon = 0.105$ and $\alpha = 1.05$ for $Re = 4000$. The constant f^* is a normalization factor so that the maximum value of $f(a.0)$ is unity and a is a root of the transcendental equation

$$\tanh(a) + \tan(a) = 0. \tag{17}$$

The above defined function belongs to a class of orthogonal functions which satisfy four boundary conditions (the function together with its first derivative vanishes at the ends of the chosen interval, i.e., at the solid walls of the plane channel in the present case). The details in the derivation of this type of functions may be found in Chandrasekhar [1, Appendix V]. Solutions of the above indicated form have been sought by George *et al.* [7] using a spectral method [6]. They have found that the fluctuation amplitude of the disturbance shows a small decay followed by a sustained slow growth. This behavior hoists up this test to a very effective estimation of the damping and phase accuracy inherent to a particular numerical scheme [5].

4 Results

The numerical simulation of a small-amplitude disturbance has been performed using the three finite difference schemes already described, employing three computational grid sizes. The numerical grid is equispaced in the streamwise direction but stretched in the wall-to-wall direction. The stretching of the mesh was obtained through a mild geometric progression (an expansion rate of 1.05 was employed).

Figure 1 shows the behavior of the perturbation energy in the channel, given by equation (14), as a function of the non-dimensional time. The (exact) solution from LST corresponds to the solid line, showing an amplification of about one order of magnitude during the simulation time. For a (16×65) computational grid, amplification was obtained only for scheme C. However, it can be seen that too much dissipation occurs. When a (32×65) grid was used, amplification of the initial disturbance occurred for all the three schemes. Yet, whereas scheme C complies with the exact solution for the actual spatial resolution, this grid still demonstrates inadequacy for schemes A and B, which exhibit considerable damping errors. Employing these latter two schemes, a (64×65) grid was found to be required for the reproduction of the LST solution.

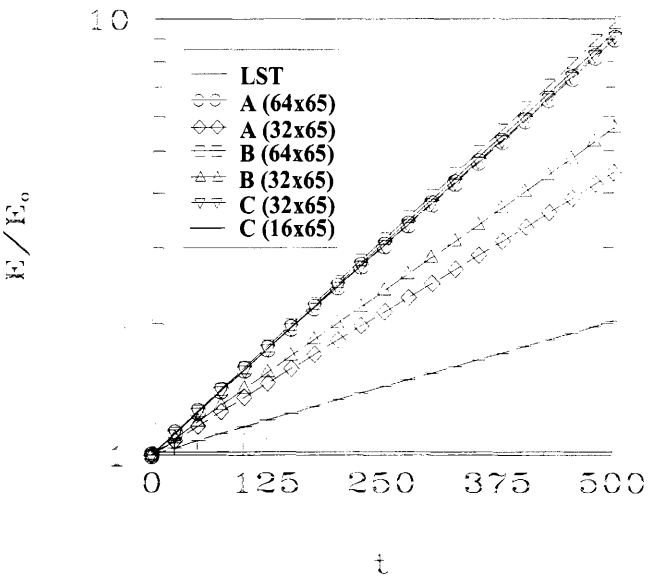

Figure 1: Energy growth rates for the numerical schemes.

Based on the results provided by this preliminary test, the computational meshes to be used in the simulation of the proposed finite-amplitude disturbance problem have been selected. Therefore, a (32×65) grid will be used in conjunction with scheme C, while (64×65) control vol-

umes are expected to be required for an accurate simulation when schemes A and B are employed.

The finite-amplitude disturbance simulations have been performed following the strategy delineated in Subsection 3.2. As mentioned earlier, the results reported by George *et al.* [7] will be used as reference solution.

Figure 2 displays the results obtained with scheme A. It can be observed that the numerical method is very much demanding in terms of the Courant number. In fact, this parameter had to be reduced to very small values ($C = 0.05$) before the method could produce acceptable results. For the chosen spatial resolution, numerical dissipation and dispersion are seen to seriously corrupt the solution when the Courant number is increased. Actually, for Courant numbers above 0.2, sustained growth of the disturbance could not be obtained employing this method.

The results obtained with scheme B are portrayed in Figure 3. In contradistinction to scheme A, scheme B is much less stringent with respect to the time step. The Courant number could be increased up to $C = 0.4$ without resulting in any noticeable change in the computations. The comparison of the behavior of the present solution with the one reported by George *et al.* [7, Figure 1], clearly shows that the temporal and spatial resolution are adequate to accurately resolve the present flow problem. Gao and Leslie [5] have also performed these same calculations utilizing a similar numerical discretization. Our results employing the (64×65) grid are clearly less damped and show a larger phase change in the period of simulation than the ones reported by the mentioned authors. However, they have used a spatial resolution of (32×64) grid nodes only (actually the computational mesh was $(32 \times 4 \times 64)$). For this reason, the results of a sample computation using a (32×65) grid were included in Figure 3. These compare well with the results of Gao and Leslie [5], unequivocally indicating inadequate spatial resolution.

Figure 4 shows the results produced by the application of scheme C. It has been observed that, for the present scheme, a spatial resolution of (32×65) is sufficient to yield accurate results. Further, the simulations were found to be nearly insensitive to the Courant number, up to $C = 0.4$.

Finally, Figure 5 summarizes the results obtained employing the three numerical schemes under scope, for a realistic Courant number ($C = 0.2$) if one bears in mind the aim of carrying out real fluid flow calculations. The solutions obtained with scheme B are very close to those generated by scheme C, but they require the double of control volumes.

5 Conclusions

An accuracy comparison of high-order finite difference schemes has been performed. The first scheme (QUICKEST) employed a quadratic Leith-type of temporal discretization together with the third-order accurate QUICK formulas for the approximation of the convective terms. The second scheme used the same spatial discretization but the time-stepping procedure was constructed using the Crank-Nicholson/Adams-Bashforth method. In the third scheme, Adams-Bashforth was used again for the time advancement of variables; fourth-order accuracy was required for spatial discretization but, for the convective terms, fifth-order accurate upwind-biased differences were used.

The finite difference methods were evaluated using two test cases: the evolution of small- and finite-amplitude disturbances in spatially periodic plane channel flow. The results obtained for these test cases allowed to quantify the grid and time-step requirements in order to obtain accurate results. As a reference for the comparison, linear stability theory and spectral method solutions have been used. The following conclusions were drawn:

1. For the same spatial resolution, the QUICKEST scheme required very low Courant numbers ($C \leq 0.05$) to avoid that damping and phase errors corrupted the solution;

2. The second scheme has shown to be insensitive to the Courant number (at least up to $C = 0.4$; however, the method is still quite demanding with respect to grid requirements, as accurate results could only be produced employing a (64×65) computational grid;

3. The third finite difference scheme investigated in the present work demonstrated the ability to accurately perform the simulations embraced by the test cases employing only 50% of the control volumes required by the remaining methods; small sensitivity to the Courant number effect was also apparent from the simulations reported herein.

References

[1] S. Chandrasekhar, *Hydrodynamic and hydromagnetic stability*, Oxford University Press, 1961.

[2] S.I. Cheng, *Accuracy of difference formulation of Navier-Stokes equations*, A.M.S. Department, Princeton University, Princeton, New Jersey, 1968.

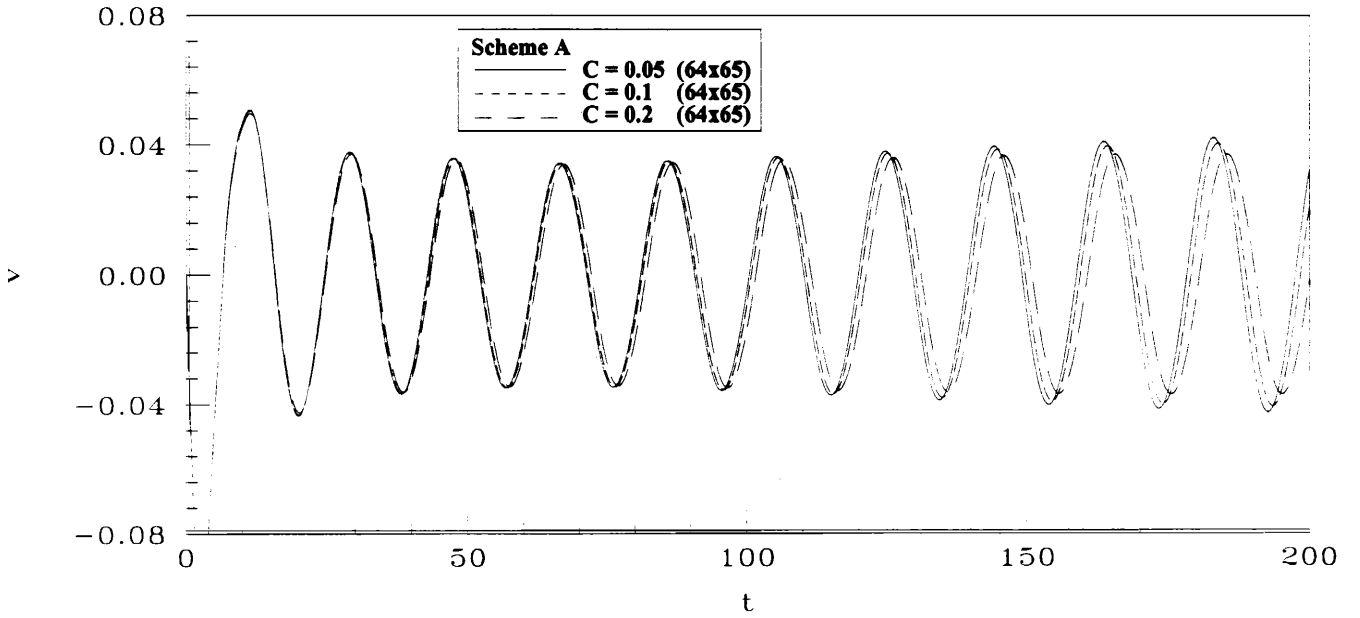

Figure 2: Temporal evolution of the v-velocity component for scheme A.

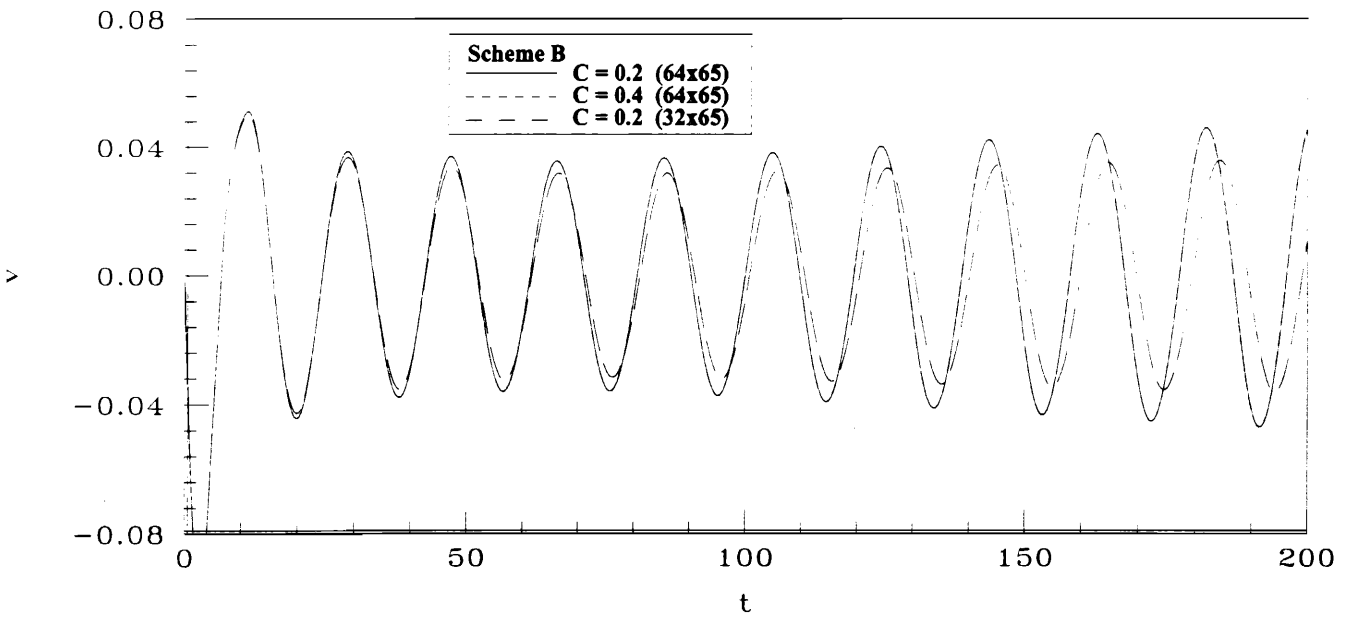

Figure 3: Temporal evolution of the v-velocity component for scheme B.

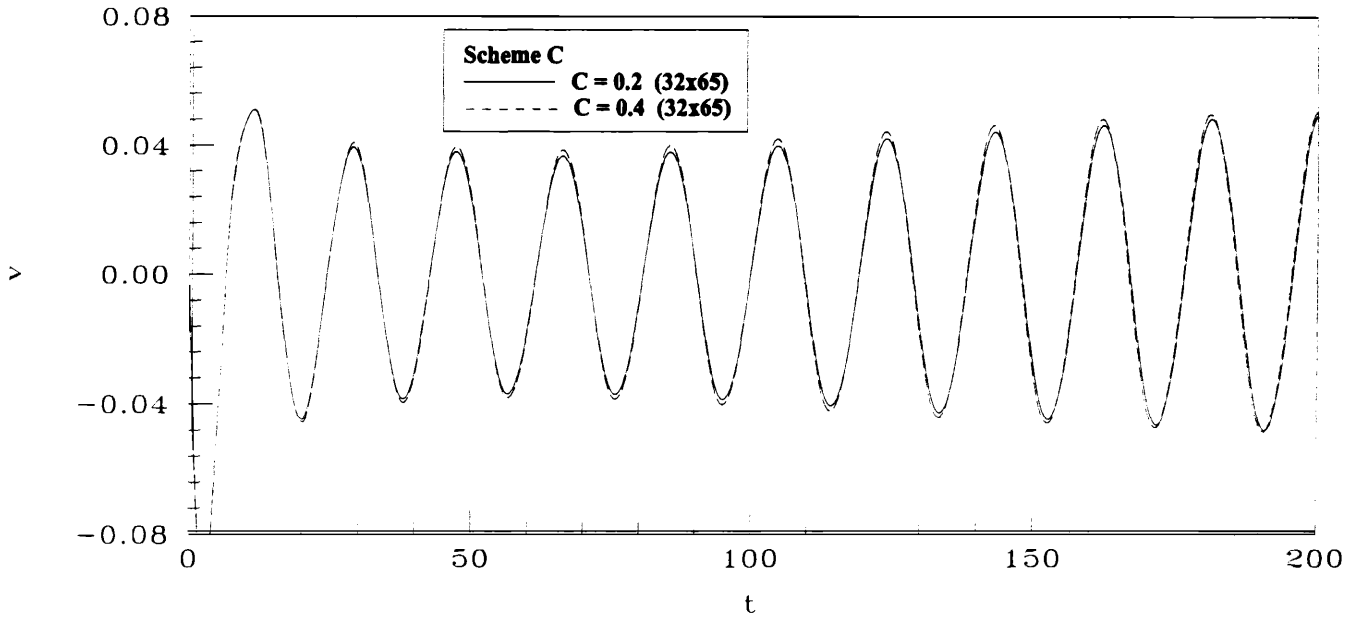

Figure 4: Temporal evolution of the v-velocity component for scheme C.

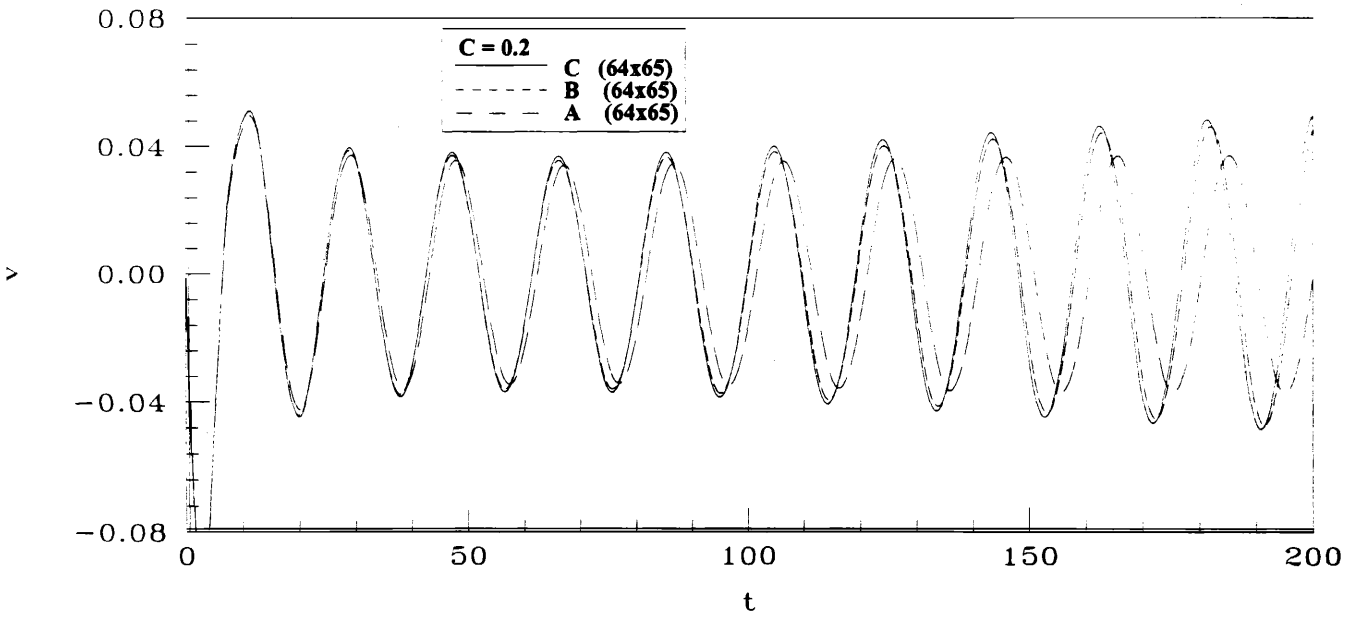

Figure 5: Temporal evolution of the v-velocity component for all schemes with $C = 0.2$.

[3] H. Fasel, *Investigation of the stability of boundary layers by a finite-difference model of the Navier-Stokes equations*, J. Fluid Mech., 78 (1976), pp. 355–383.

[4] H. Fasel, *Recent developments in the numerical solution of the Navier-Stokes equations and hydrodynamic stability problems*, Lecture Notes VKI, Lecture Notes in Computational Fluid Dynamics, Hemisphere Corporation, 1978.

[5] S. Gao and D.C. Leslie, *Accuracy comparison of Adams-Bashforth and leapfrog in context of large eddy simulation*, Commun. Appl. Numer. Methods, 6 (1990), pp. 1–5.

[6] W.D. George and J.D. Hellums, *Hydrodynamic stability in plane Poiseuille flow with finite amplitude disturbances*, J. Fluid Mech., 51, 4 (1972), pp. 687–704.

[7] W.D. George, J.D. Hellums and B. Martin, *Finite-amplitude neutral disturbances in plane Poiseuille flow*, J. Fluid Mech., 63, 4 (1974), pp. 765–771.

[8] J. Jiménez. *Transition to turbulence in two-dimensional Poiseuille flow*, J. Fluid Mech., 218 (1990), pp. 265–297.

[9] B.P. Leonard, *A stable and accurate convective modelling procedure based on quadratic upstream interpolation*, Comput. Methods Appl. Mech. Engrg., 19 (1979), pp. 59–98.

[10] M.R. Malik, T.A. Zang and M.Y. Hussaini, *A spectral collocation method for the Navier-Stokes equations*, J. Comput. Phys., 61, 1 (1985), pp. 64–88.

[11] S.A. Orszag, *Accurate solution of the Orr-Sommerfeld stability equation*, J. Fluid Mech., 50 (1971), pp. 689–703.

[12] S.A. Orszag and L.C. Kells, *Transition to turbulence in plane Poiseuille and plane Couette flow*, J. Fluid Mech., 96, 1 (1980), pp. 159–205.

[13] S.A. Orszag and A.T. Patera, *Subcritical transition to turbulence in plane channel flows*, Phys. Rev. Lett., 45, 12 (1980), pp. 989–993.

[14] S.A. Orszag and A.T. Patera, *Secondary instability of wall-bounded shear flows*, J. Fluid Mech., 128 (1983), pp. 347–385.

[15] A.T. Patera and S.A. Orszag, *Finite-amplitude stability of axisymmetric pipe flow*, J. Fluid Mech., 112 (1981), pp. 467–474.

[16] J.C.F. Pereira and J.M.M. Sousa, *Finite volume calculations of self-sustained oscillations in a grooved channel*, J. Comput. Phys., 106 (1993), pp. 19–29.

[17] M.M. Rai and P. Moin, *Direct simulations of turbulent flow using finite-difference schemes*, J. Comput. Phys., 96 (1991), pp. 15–53.